In vivo assessment of the vascular disrupting effect of M410 by DCE-MRI biomarker in a rabbit model of liver tumor

RUI-MENG YANG[1], YONG ZOU[2], DAN-PING HUANG[1], SHENG-SHENG LAI[3], XIANG-DONG XU[1], XIN-HUA WEI[1], HAN-ZHENG CHANG[1], TONG-KUN HUANG[2], LI WANG[1], WEN-JIE TANG[1] and XIN-QING JIANG[1]

[1]Department of Radiology, Guangzhou First People's Hospital, Guangzhou Medical University, Guangzhou 510180; [2]Guangzhou Institute of Chemistry, Chinese Academy of Science, Guangzhou 510650; [3]Department of Medical Equipment, Guangdong Food and Drug Vocational College, Guangzhou 510520, P.R. China

Received February 18, 2014; Accepted April 7, 2014

DOI: 10.3892/or.2014.3230

Abstract. The present study aimed to prospectively monitor the vascular disrupting effect of M410 by dynamic contrast-enhanced magnetic resonance imaging (DCE-MRI) in rabbits with VX2 liver tumors. Twenty-eight rabbits bearing VX2 tumors in the left lobe of the liver were established and randomly divided into treatment and control groups, intravenously injected with 25 mg/kg M410 or sterile saline, respectively. Conventional and DCE-MRI data were acquired on a 3.0-T MR unit at pretreatment, 4 h, 1, 4, 7 and 14 days post-treatment. Histopathological examinations [hematoxylin and eosin (H&E) and CD34 immunohistochemisty staining] were performed at each time point. The dynamic changes in tumor volume, kinetic DCE-MRI parameter [volume transfer constant (K^{trans})] and histological data were evaluated. Tumors grew slower in the M410 group 4-14 days following treatment, compared with rapidly growing tumors in the control group ($P<0.05$). At 4 h, 1 and 4 days, K^{trans} significantly decreased in the M410 group compared with that in the control group ($P<0.05$). However, K^{trans} values were similar in the two groups for the other time points studied. The changes in DCE-MRI parameters were consistent with the results obtained from H&E and CD34 staining of the tumor tissues. DCE-MRI parameter K^{trans} may be used as a non-invasive imaging biomarker to monitor the dynamic histological changes in tumors following treatment with the vascular targeting agent M410.

Introduction

Vascular disrupting agents (VDAs) have emerged as a new class of anticancer drugs in recent years (1). These therapeutics take advantage of the weakness of established tumor endothelial cells and their supporting structures. In contrast to antiangiogenic therapy, which inhibits the outgrowth of new blood vessels, vascular targeting treatments selectively attack the existing tumor vasculature and cause vascular shutdown in preexisting tumor vessels by a preferential effect on the tumor. Combretastatin A-4-phosphate (CA4P) is one of the most representative VDAs and it is well known that structural modification is an effective approach for developing new agents with higher activity with less adverse reactions. Compound M410, a new combretastatin derivative with vascular disrupting properties, has been shown in a previous study to exhibit pronounced inhibitory effects on proliferation of tumor cells and HUVECs (1). Therefore, we chose this compound for the present study.

In order to realize 'personalized medicine' and monitor early hemodynamic alterations, cellular dysfunctions and metabolic impairments before tumor dimensional changes can be detected, early and non-invasive diagnosis using imaging biomarkers as a surrogate end point becomes clinically pivotal for therapeutic assessment. Such information allows for discrimination of responders from non-responders to justify the individualized therapeutic regimen (2).

Dynamic contrast-enhanced MR imaging (DCE-MRI) is a non-invasive imaging technique capable of characterizing tissue vasculature, sensitive to differences in blood volume and vascular permeability potentially related to tumor angiogenesis (3). Therefore, DCE-MRI has the potential to evaluate the therapeutic response to antiangiogenic treatments. Herein, we conducted a study to prospectively monitor changes in volume and transfer constant (K^{trans}) in M410 vascular disruption of rabbit liver tumors. VX2 carcinoma implanted in rabbit liver was used in the present study, a well-established model for investigation of chemotherapy agents and their bioavailability, similar to human hepatomas (4-6). We aimed to use DCE-MRI as a non-invasive marker to test the vascular disrupting agent M410.

We found that tumors grew slower 4-14 days following M410 treatment. At earlier time points (4 h to 4 day), K^{trans} was significantly reduced in the M410 group compared with the controls. The changes observed in DCE-MRI parameters were

Correspondence to: Dr Xin-Qing Jiang, Department of Radiology, Guangzhou First People's Hospital, Guangzhou Medical University, Guangzhou 510180, P.R. China
E-mail: jiangxinqing888@163.com

Key words: dynamic contrast-enhanced MRI, neoplasms, molecular targeted therapy, response monitoring, M410

consistent with histological data obtained after hematoxylin and eosin (H&E) staining and CD34 histochemistry. These findings suggest that the DCE-MRI parameter K^{trans} may be used as a non-invasive imaging biomarker to monitor the dynamic histological changes in tumors after treatment with vascular targeting agents.

Materials and methods

Animals and tumor model. This animal study was in compliance with national and international regulations and was approved by the Institutional Ethics Committee for Animal Care and Use. Twenty-eight male New Zealand white rabbits (weight, 2.0-2.5 kg) were used in these experiments. VX2 carcinomas were implanted in rabbit livers (4-6) used in the present study. The New Zealand white rabbits and the VX2 tumor masses were provided by the Center of Laboratory Animal Science of Guangdong.

Experimental drug. The new compound M410 (patent no. ZL20061003378.1), a combretastatin derivative vascular disrupting agent, was synthesized according to previously published procedures by the Guangzhou Institute of Chemistry, Chinese Academy of Sciences (7). The chemical structure of (Z)-3,4',5-trimethoxylstilbene-3'-O-phosphate disodium (M410) is shown in Fig. 1.

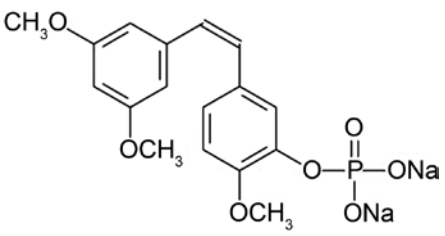

Figure 1. Chemical structure of M410.

Table I. Parameters used for conventional MRI assays.

	T1WI	T2WI	DCE-T1
Sequence type	FLASH	TSE	VIBE
Repetition time (msec)	120	3158	4.9
Echo time (msec)	3.5	61	1.9
Flip angle (degrees)	180	180	180
Field of view (mm^2)	65x65 mm	65x65 mm	240x240 mm
Slice thickness (mm)	3	3	3

MRI, magnetic resonance imaging; T1WI, T1-weighted imaging; T2WI, T2-weighted imaging.

Experimental protocol. Rabbits were randomly assigned to the M410 treatment (n=14) or the control (n=14) group. M410 was dissolved in 2 ml sterile saline and administered by marginal ear vein injection at a dose of 25 mg/kg every three days during the experiment; while equal volumes of sterile saline were intravenously administered to control animals. MRI was performed pre-treatment, and 4 h, 1 d, 4 d, 7 d and 14 d following initial treatment (Fig. 2). For postmortem verification of the imaging findings, 2 rabbits were sacrificed per group for histopathological examinations (H&E staining and CD34 immunohistochemisty) at each time point immediately after MR scan.

Magnetic resonance assays. MRI examinations were performed on a 3.0-Tesla MR system (Verio; Siemens, Erlangen, Germany) with a soft coil. The protocols for conventional MRI consisted of a three-plane localizer, axial T1-weighted, axial and coronal T2-weighted sequences (Table I).

DCE-MRI was performed using the following sequences: two precontrast datasets were acquired using T1-weighted MRI (TR/TE, 120/3.5 msec; FOV, 65x65 mm), followed by a DCE acquisition series using the T1-twist (TR/TE, 4.9/1.9 msec; FOV, 240 x 240 mm). After fifth baseline acquisition, a gadolinium (Gd)-based contrast agent, Gd-diethylenetriamine pentaacetic acid (Gd-DTPA) was injected through the marginal ear vein as a bolus at 4 ml/sec and a dose of 0.1 mmol/kg of body weight, immediately followed by a 10-ml saline flush.

MRI analyses. All MRI analyses were performed by two experienced radiologists and consensus was reached for each case.

Tumor volume measurements were performed with Syngo MR (Siemens). On T2WI, the tumor area was manually delineated with a freehand region of interest (ROI) on all tumor-containing images. The total tumor volume was calculated using the following equation:

$$\sum \text{Tumor area on each tumor-containing slice} \times (\text{slice thickness} + \text{gap}) \quad [1]$$

DCE-MRI analysis was performed using the Tissue 4D software (Siemens) included on a Siemens syngo MR workstation. The map of K^{trans}, volume transfer constant per unit volume of tissue (unit/min), was generated by fitting the Tofts and Kermode model (8). Pharmacokinetic modeling is based on the assumption that contrast agents exist in two interchanging compartments (plasma and EES). Free-hand ROIs were used to delineate the entire tumor on the corresponding axial post-contrast T1-weighted MRI and automatically transferred onto parametric maps. The ROI was along the edge of the enhanced-tumor on all tumor-containing image slices of the

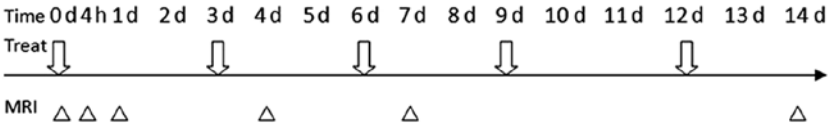

Figure 2. Treatment schedule and MRI imaging sessions. MRI, magnetic resonance imaging.

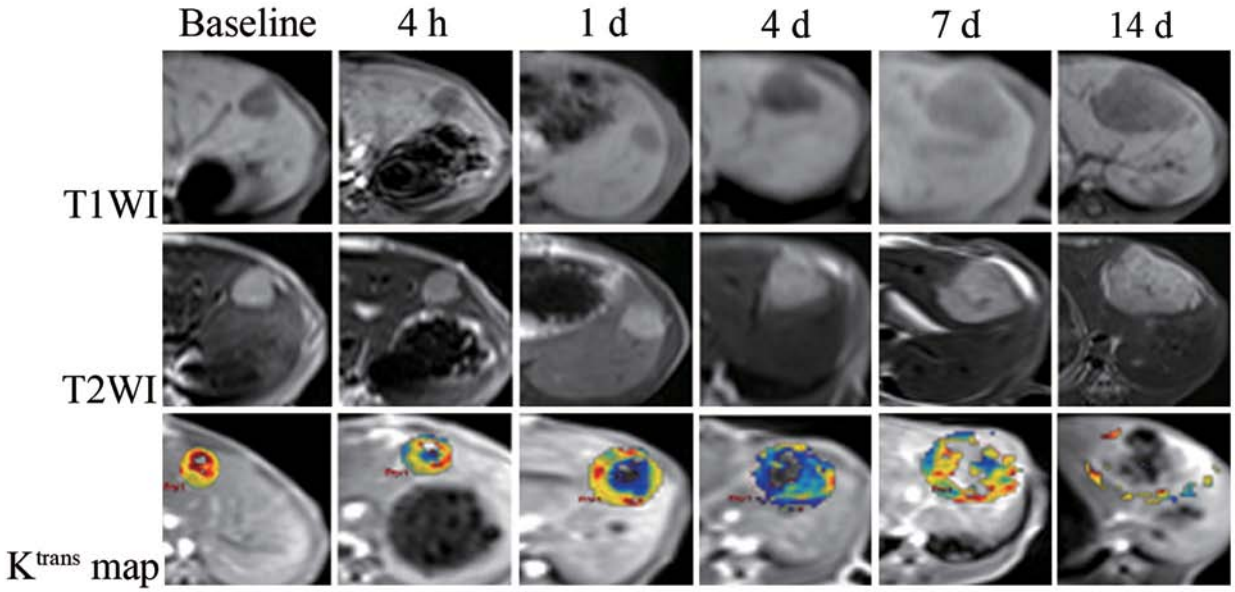

Figure 3. Findings in the M410 group. At all time points, the tumor was hypointense on T1-weighted imaging (T1WI) and heterogeneously hyperintense on T2-weighted imaging (T2WI). On the volume transfer constant (K^{trans}) map, the tumor showed abundant blood supply with high K^{trans} before treatment. At 4 h, 1 and 4 days after VDA treatment, vascular shutdown was indicated by low K^{trans} in the tumor. At 7-14 days after treatment, K^{trans} remained low with the tumor showing rebounding of K^{trans}. VDA, vascular disrupting agents.

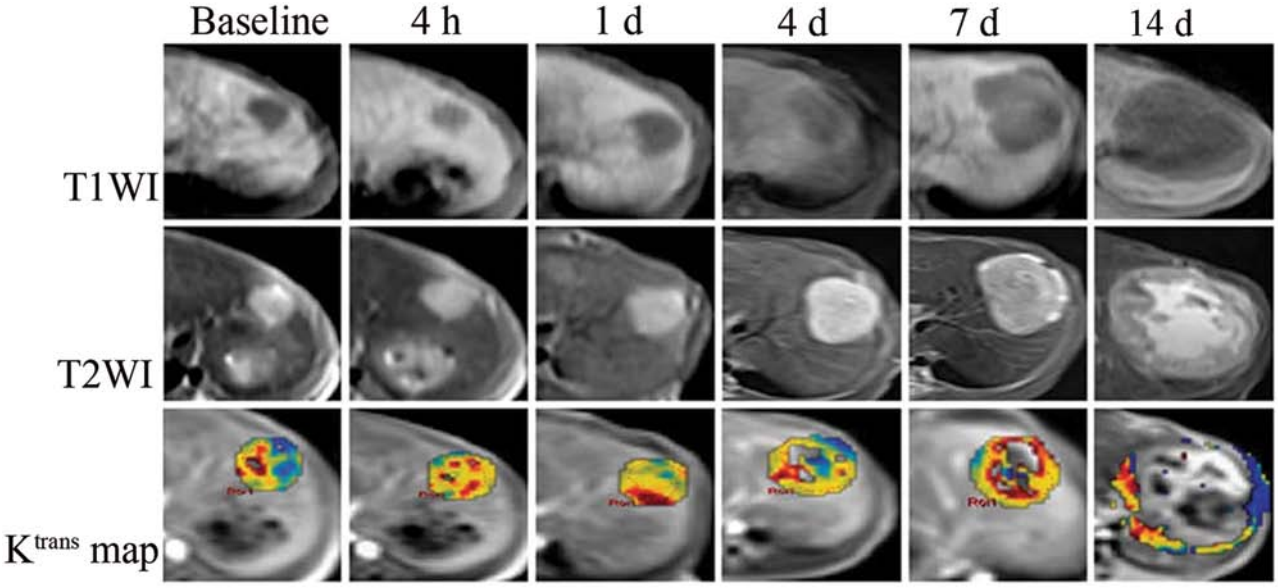

Figure 4. Findings in the control group. The tumor remained hypointense on T1-weighted imaging (T1WI) at all the time points. Likewise, the tumor was hyperintense on T2-weighted imaging (T2WI) throughout the experiment, with obvious liquefaction necrosis in the center of tumor at 14 days. On the volume transfer constant (K^{trans}) map, the tumor showed abundant blood supply with high K^{trans} throughout the experiment.

parametric images. Averages and standard deviations for K^{trans} were calculated for each group at each time point for statistical analysis. Tumor K^{trans} change (%) at various time points after treatment was defined as follows:

K^{trans} (post-treatment) - K^{trans} (baseline)/K^{trans} (baseline) x 100% [2]

Histology and immunohistochemistry. The rabbits were sacrificed immediately after the MR scan by air embolism after injection of 10-20 ml air via the marginal ear vein. The liver lobe with the tumor was cut into 5-mm-thick blocks to match the sections from the DCE-MR study, fixed in 10% formaldehyde, embedded in paraffin and cut into 5-μm-thick slices, and submitted to H&E staining and $CD34^+$ immunohistochemistry. Sections were observed microscopically for assessment of viable tumor cells, interstitium, necrosis and tumor vasculature. Finally, histological sections were visually compared with the corresponding conventional images and the K^{trans} maps.

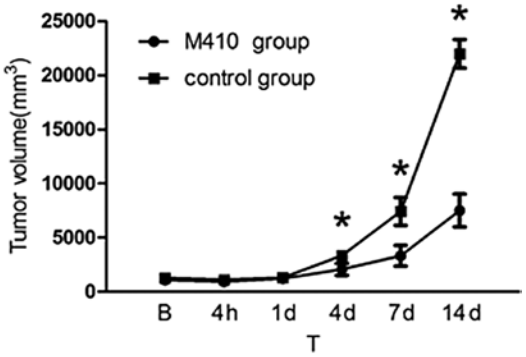

Figure 5. Comparison of tumor volumes between the M410 and control group at different time points. The line chart shows that the mean tumor volume increased faster in the controls than that in the M410-treated animals. At 4-14 days, the tumors were significantly larger in the control animals than in the M410 group.

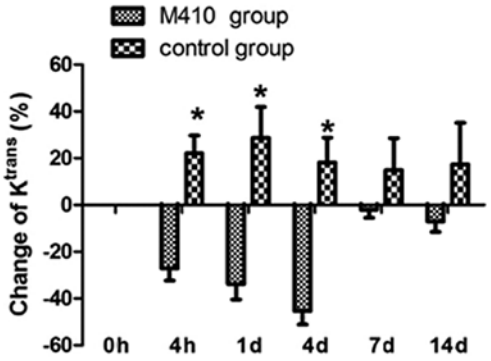

Figure 6. Comparison of tumor K^{trans} change (%) between the M410 and control group at different time points. The tumor K^{trans} change (%) revealed vascular shutdown at 4 h until 4 days, with partial recovery at 7 and 14 days.

Statistical analyses. Statistical analyses were carried out using Microsoft Office Excel 2007 and the Statistical Package for the Social Sciences 16.0 (SPSS, Chicago, IL, USA). Data are reported as means ± standard deviation. Tumor volume, K^{trans} and the percentile change in K^{trans} at various time points between the control and M410 group after treatment were compared by two-tailed Student's t-test. A significant difference was concluded for a P-value of <0.05.

Results

General conditions and conventional MRI findings at baseline. All rabbits survived the entire experimental procedure including anesthesia, tumor implantation and growth, and MRI sessions. The liver tumor model was successfully established in all rabbits. They tolerated the intravenous administration of M410 well without detectable side-effects.

At baseline, the tumors showed an oval shape with a clear border easily demarcated from the adjacent normal liver tissue with all imaging sequences. The tumor appeared hyperintense on T2WI and hypointense on T1WI. In the center of several tumors, minute dots or irregular foci of necrosis were noticed, which appeared more hyperintense and hypointense on T2- and T1-weighted images.

Comparison of the therapeutic effects. Following VDA treatment, a number of T2WI and T1W MRI results revealed evidence of hemorrhage. M410 caused rapid vascular shutdown in tumors, induced tumor necrosis and delayed tumor growth compared with the controls (Figs. 3-6). However, tumor blood supply gradually rebound even after repeated VDA treatment, resulting in tumor recurrence at the periphery.

Tumor volume assessment. There was no significant difference in tumor volume between the two treatment groups at baseline (1,076±613 mm^3 in the M410 group vs. 1,273±334 mm^3 in the control group, P>0.05), 4 h (927±472 vs. 1,108±200 mm^3, P>0.05) and day 1 (1,218±939 vs. 1,308±284 mm^3, P>0.05). With time, tumor growth was observed in both groups, although tumors in the control animals grew faster: 4 days (2,063±1,541 vs. 3,350 mm^3, P<0.05); 7 days (3,325±2,328 vs. 7,421±3,177 mm^3, P<0.05); 14 days (7,518±3,045 vs. 22,000±2,653 mm^3, P<0.05). These data showed significantly larger mean tumor volumes in the controls compared with the M410-treated animals, indicating that M410 overtly inhibits tumor growth (Fig. 5).

Quantitative assessment of therapeutic effect using K^{trans}. Before treatment, no significant difference was observed in tumor K^{trans} values between the M410-treated and control animals, with 0.315±0.044 and 0.323±0.496/min recorded for the control and M410 groups, respectively (P>0.05).

Following treatment with M410, rapid vascular shutdown in tumors and induced tumor necrosis occurred, resulting in decreased K^{trans}. In the M410 group, K^{trans} decreased from 4 h to 4 days after the first administration, and partially recovered at 7 and 14 days time points. Indeed, K^{trans} was significantly reduced after M410 treatment in comparison with the control animals at 4 h (0.233±0.098/min in the M410 group vs. 0.374±0.060/min in the controls, P<0.05), 1 day (0.215±0.069 vs. 0.385±0.100/min, in M410 and control groups, respectively, P<0.05) and 4 days (0.176±0.044 vs. 0.347±0.070/min, in the M410 and control groups, respectively, P<0.05). Of note, K^{trans} was not significantly different between the M410 and saline-treated animals at the other time points studied.

After standardization, the percentile change in K^{trans} was zero both in the M410 and control groups at baseline. After M410 administration, similar to the K^{trans} trend, the percentile changes in K^{trans} revealed vascular shutdown at 4 h to 4 days, with partial recovery at 7 and 14 days (Fig. 6).

Effect of M410 on tumor cells and vessels as evaluated by histology. Four hours and 1 day after administration of M410, the membranes of most of the cells were still intact under light microscopy, despite the heavy edema detected in tumors. At 4 days, H&E-stained sections showed large necrotic areas, which were unanimously identified as eosinophils. Viable tumor cells were noted only in the outer peripheral rims. Seven and 14 days after M410 treatment, liver sections showed central necrosis mixed with re-growing tumor. Histology and immunostained sections of tumors from the control animals revealed poorly differentiated tumor cell histology with distinctly visible $CD34^+$ endothelial cells. In sharp contrast, minimal CD34 staining with irregular endothelial fragments

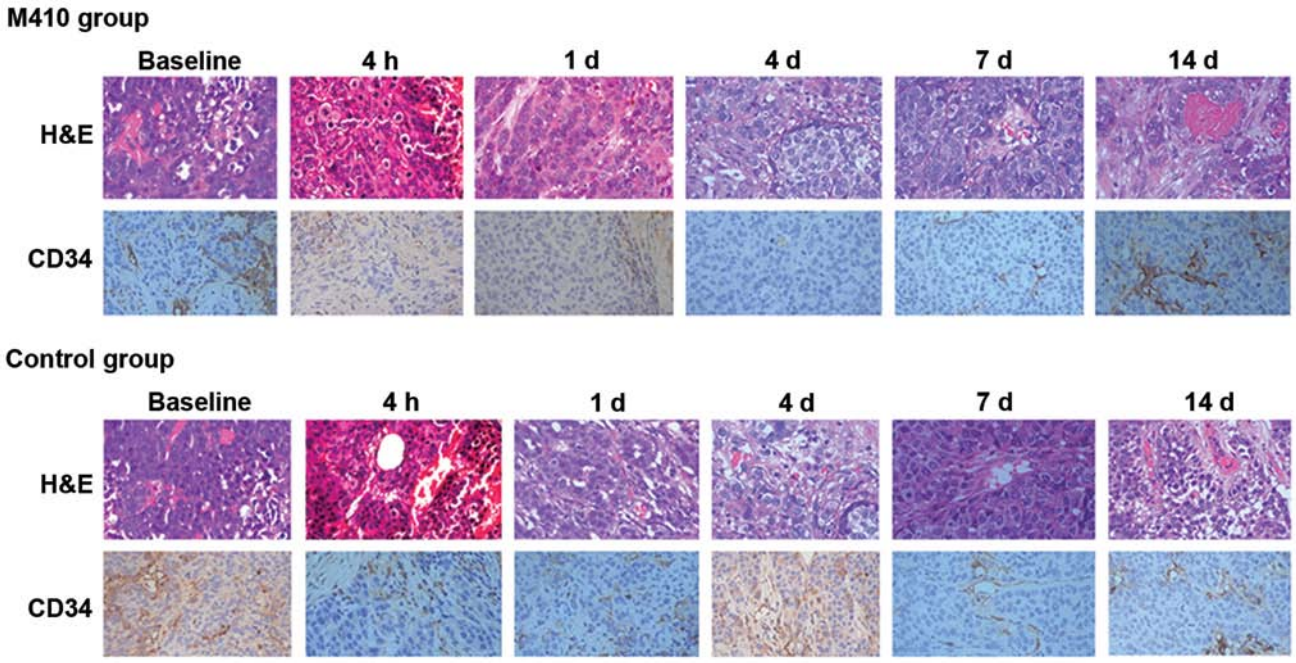

Figure 7. Morphological changes in tumor vessels induced by M410 treatment. Tumor paraffin sections were stained with H&E or antibodies raised against CD34. Representative micrographs for each group at each time point. Magnification, x400. (N, normal hepatic tissue; T, tumor). H&E, hematoxylin and eosin.

and faint outlines of blood vessels were observed in the M410-treated tumors at 4 h, 1 and 4 days post-treatment (Fig. 7), with partial recovery 7 and 14 days after the first administration. Importantly, liver vessels were not inhibited by M410 treatment at any time point.

Discussion

Tumor angiogenesis is one of the hallmarks of cancer and a critical determinant of malignant progression in most solid tumors (9). Thus, tumor vasculature constitutes an attractive target for anticancer therapies. Exploiting the distinct characteristics between tumor and normal vessels, vascular disrupting agents (VDAs) selectively destroy tumor vessels and cause rapid vascular shutdown, resulting in extensive ischemic tumor necrosis, with normal vessels less affected. Although not fully understood, one of the mechanisms underlying VDA action is probably inhibition of tubulin polymerization.

CA4P, one of the most potent VDAs, has been characterized for its selective tumor vascular targeting effects, both *in vivo* and *in vitro*. Indeed, it was found that tumors grow slower in rats treated with CA4P with a high necrosis ratio at 5 days. In addition, volume transfer constant values in the CA4P group decreased from 1 until 6 h, and partially recovered at 5 days (2). The newly designed combretastatin derivative vascular disrupting agent, compound M410, is a verified potent microtubule inhibitor with cytotoxic activity, inhibiting angiogenesis and targeting tumor vessels (1). In this study, we prospectively monitored the vascular disrupting effect of M410 in rabbit liver tumors.

Current conventional imaging techniques rely on identifying morphologic criteria as well as changes in tumor dimensions to evaluate and monitor therapeutic response or disease progression, which led to the emergence of response criteria such as those proposed by the Response Evaluation Criteria in Solid Tumors (RECIST) Committee (10). However, with the increasing clinical use of cytostatic or molecular targeted therapeutics, there is a recognition that anatomic evaluations are insensitive to changes that may inform on overall therapeutic success. In the present study, M410 reduced tumor growth, but the significance was reached only until 4 days, also suggesting that the value of anatomic imaging as a surrogate marker of clinical efficacy for antiangiogenic therapies may be limited.

Currently, multiparametric MRI biomarkers are able to non-invasively probe the early vascular properties during VDA treatment with qualitative and quantitative evaluation of morphological, functional and metabolic/molecular changes (11,12). Among MRI biomarkers, DCE-MRI remains a promising biomarker for assessing antiangiogenic therapy (11). DCE-MRI involves the acquisition of sequential images during the passage of a contrast agent through a particular tissue of interest (13). Relevant pharmacokinetic modeling parameters can also be determined for a defined region of interest on the image of choice, further allowing integration of function and form (11). In this study, we chose the Tofts two-compartment pharmacokinetic model (13), and the physiological parameter K^{trans} was returned. K^{trans} is the rate of flux of the contrast agent from plasma into extravascular extracellular space (EES), and can be used to quantify the permeability of tumor vessels. Before treatment, tumor vessels are highly permeable and therefore blood flow dominates K^{trans}, meaning that K^{trans} is more perfusion weighted. Upon treatment, both blood flow and the functional endothelial surface area are reduced and K^{trans} mirrors the combination of blood flow and permeability surface area product (14). Our data showed a significant decrease in K^{trans} in the M410-treated animals compared with controls at 4 h, 1 and 4 days.

A single VDA dose has been demonstrated to induce vascular damage and perfusion changes in tumors although its efficacy varies significantly among different types of tumors (15). Moreover, regardless of the degree of vascular damage, the drug has only a slight impact on tumor growth. It is well known that continual growth of a tumor is attributed to an actively proliferating population of cells at the tumor periphery, which receives their nutritional support, at least in part, from normal vessels in the surrounding host tissue. Therefore, a substantial effect is generally observed in central tumor regions after treatment with VDAs, whereas peripheral tumor cells are unaffected and form a viable rim. To deal with this limitation and improve the therapeutic effect of VDAs, measures such as adjuvant conventional cytotoxic approaches or radiation therapies are undertaken (16). Interestingly, repeated drug administration at time intervals appears more effective (17). Therefore, a regimen of repeated intravenous injections (every three days) was chosen to investigate the M410 vascular disrupting effect on solid tumors *in vivo*, and we demonstrated that at a clinically relevant dose, M410 caused selective vascular shutdown in rabbit liver tumors. The degree in the drop in blood supply with M410 reflected by K^{trans} was observed 4 h after treatment, and continued for 4 days. From 7 days onwards, the blood flow at the tumor periphery started to regain strength and central necrosis developed, leading to elevated K^{trans}. The number of tumor vessels identified by CD34 staining in the tumors as a whole decreased 4 h following treatment, and subsequently recovered after 7 days. Several studies have shown that tumor blood supply is compromised within minutes after a single treatment dose of VDAs (18,19). The duration of inhibition of functional blood vessels may depend on VDA dose and tumor model. In the present study, the vascular shutdown effect was detected with the imaging biomarker K^{trans} from 4 h to 4 days after treatment with M410. The extension of vascular shutdown duration may result from the regimen of repeated intravenous injections.

Many reasons may explain the presence of a viable rim of tumor cells surviving at the periphery either after single or repeated-dose VDA treatment. First, cells at the tumor periphery can directly obtain nutrients and oxygen from neighboring normal host tissues and engulf normal vessels during rapid tumor growth (20). Another possible reason may be the post-treatment changes in tumor phenotype (21). Hypoxic conditions in the tumor after VDA treatment may upregulate hypoxia-inducible factor 1α (HIF-1α), stimulate the expression of angiogenic genes, increase vascular endothelial growth factor (VEGF) levels, and enhance the angiogenesis process. Therefore, neoangiogenesis is accelerated in the tumors after VDA treatment (21-23). This explains why tumor growth is only delayed and not destroyed (24,25). Based on the aforementioned limitations of VDA, vascular disrupting agents may be more effective to treat cancer in combination with other chemotherapeutic agents. Liver X receptors (LXRs) are important nuclear receptors which include LXRα and LXRβ (26,27). Activation of LXRs can inhibit cell proliferation and suppress progressive cancer properties such as invasion, angiogenesis and metastasis in multiple human cancers (28,29). Therefore, the efficacy of vascular disrupting agents combined with agonists for LXRs will be investigated in our future research using a rabbit model of liver tumor.

There are some limitations to this study. First, the image analyses in DCE-MRI were performed on whole tumors. Due to the treatment resistance, there was always a tumor residue at the periphery surrounding the necrotic center. Such heterogeneity of the tumor response to VDAs was not analyzed on a pixel-by-pixel basis. Characterization of a heterogeneous response in the tumor may provide more predictable information regarding prognosis (30,31). Second, the changes within several hours or minutes after treatment were not monitored by MR and histology. Third, the animal tumor model may differ from humans, thus the results may not be completely representative of the imaging or histological features of cancer patients.

In conclusion, at a clinically relevant repeated dose, M410 proved to be an effective VDA inducing vascular shutdown in rabbit VX2 liver tumors, although tumor re-growth at the periphery inevitably led to tumor recurrence. The dynamic histological changes in tumors caused by M410 as precisely reflected by DCE-MRI with the K^{trans} biomarker indicate a non-invasive and quantitative measure for monitoring tumor vascular targeting treatment.

Acknowledgements

This study was supported by the National Natural Science Foundation of China (81201087), and the Natural Science Foundation of Guangdong Province, China (10151006001000010).

References

1. Cai YC, Zou Y, Ye YL, *et al*: Anti-tumor activity and mechanisms of a novel vascular disrupting agent, (Z)-3,4',5-trimethoxylstilbene-3'-O-phosphate disodium (M410). Invest New Drugs 29: 300-311, 2011.
2. Wang H, Miranda Cona M, Chen F, *et al*: Comparison between nonspecific and necrosis-avid gadolinium contrast agents in vascular disrupting agent-induced necrosis of rodent tumors at 3.0T. Invest Radiol 46: 531-538, 2011.
3. Kim JH, Kim CK, Park BK, Park SY, Huh SJ and Kim B: Dynamic contrast-enhanced 3-T MR imaging in cervical cancer before and after concurrent chemoradiotherapy. Eur Radiol 22: 2533-2539, 2012.
4. Stewart EE, Sun H, Chen X, *et al*: Effect of an angiogenesis inhibitor on hepatic tumor perfusion and the implications for adjuvant cytotoxic therapy. Radiology 264: 68-77, 2012.
5. Ko YH, Pedersen PL and Geschwind JF: Glucose catabolism in the rabbit VX2 tumor model for liver cancer: characterization and targeting hexokinase. Cancer Lett 173: 83-91, 2001.
6. Geschwind JF, Ko YH, Torbenson MS, Magee C and Pedersen PL: Novel therapy for liver cancer: direct intraarterial injection of a potent inhibitor of ATP production. Cancer Res 62: 3909-3913, 2002.
7. Zou Y, Wang ZX, Zhang XJ, He SJ and Lin HZ: Water soluble phosphate ester salt of (Z)-3'-hydroxy-3,4',5-trimethoxys-tilbene, and its preparation method, pharmaceutical composition and uses. Chinese Patent Office, ZL 200610033788.1.
8. Tofts PS and Berkowitz BA: Rapid measurement of capillary permeability using the early part of the dynamic Gd-DTPA MRI enhancement curve. J Magn Reson, Series B 102: 129-136, 1993.
9. Seshadri M and Toth K: Acute vascular disruption by 5,6-dimethylxanthenone-4-acetic Acid in an orthotopic model of human head and neck cancer. Transl Oncol 2: 121-127, 2009.
10. Maia AC Jr, Guedes BV, Lucas A Jr and da Rocha AJ: Diffusion MR imaging for monitoring treatment response. Neuroimaging Clin N Am 21: 153-178, 2011.
11. Harry VN, Semple SI, Parkin DE and Gilbert FJ: Use of new imaging techniques to predict tumour response to therapy. Lancet Oncol 11: 92-102, 2010.

12. Tozer GM: Measuring tumour vascular response to antivascular and antiangiogenic drugs. Br J Radiol 76 (Spec No 1): S23-S35, 2003.
13. Tofts PS, Brix G, Buckley DL, *et al*: Estimating kinetic parameters from dynamic contrast-enhanced t_1-weighted MRI of a diffusable tracer: standardized quantities and symbols. J Magn Reson Imaging 10: 223-232, 1999.
14. Collins DJ and Padhani AR: Dynamic magnetic resonance imaging of tumor perfusion. Approaches and biomedical challenges. IEEE Eng Med Biol Mag 23: 65-83, 2004.
15. Nielsen T, Murata R, Maxwell RJ, *et al*: Non-invasive imaging of combretastatin activity in two tumor models: association with invasive estimates. Acta Oncol 49: 906-913, 2010.
16. Rustin GJ, Shreeves G, Nathan PD, *et al*: A Phase Ib trial of CA4P (combretastatin A-4 phosphate), carboplatin, and paclitaxel in patients with advanced cancer. Br J Cancer 102: 1355-1360, 2010.
17. Thoeny HC, De Keyzer F, Chen F, *et al*: Diffusion-weighted magnetic resonance imaging allows noninvasive in vivo monitoring of the effects of combretastatin a-4 phosphate after repeated administration. Neoplasia 7: 779-787, 2005.
18. Ching LM, Zwain S and Baguley BC: Relationship between tumour endothelial cell apoptosis and tumour blood flow shutdown following treatment with the antivascular agent DMXAA in mice. Br J Cancer 90: 906-910, 2004.
19. Seshadri M, Spernyak JA, Maiery PG, Cheney RT, Mazurchuk R and Bellnier DA: Visualizing the acute effects of vascular-targeted therapy in vivo using intravital microscopy and magnetic resonance imaging: correlation with endothelial apoptosis, cytokine induction, and treatment outcome. Neoplasia 9: 128-135, 2007.
20. Kanthou C and Tozer GM: Microtubule depolymerizing vascular disrupting agents: novel therapeutic agents for oncology and other pathologies. Int J Exp Pathol 90: 284-294, 2009.
21. Wang H, Cona MM, Chen F, *et al*: Comparison of two vascular-disrupting agents at a clinically relevant dose in rodent liver tumors with multiparametric magnetic resonance imaging biomarkers. Anticancer Drugs 23: 12-21, 2012.
22. Sheng Y, Hua J, Pinney KG, *et al*: Combretastatin family member OXI4503 induces tumor vascular collapse through the induction of endothelial apoptosis. Int J Cancer 111: 604-610, 2004.
23. Dachs GU, Steele AJ, Coralli C, *et al*: Anti-vascular agent Combretastatin A-4-P modulates hypoxia inducible factor-1 and gene expression. BMC Cancer 6: 280, 2006.
24. Siemann DW and Shi W: Dual targeting of tumor vasculature: combining Avastin and vascular disrupting agents (CA4P or OXi4503). Anticancer Res 28: 2027-2031, 2008.
25. Murata R, Overgaard J and Horsman MR: Combretastatin A-4 disodium phosphate: a vascular targeting agent that improves that improves the anti-tumor effects of hyperthermia, radiation, and mild thermoradiotherapy. Int J Radiat Oncol Biol Phys 51: 1018-1024, 2001.
26. Tan XJ, Dai YB, Wu WF, *et al*: Anxiety in liver X receptor beta knockout female mice with loss of glutamic acid decarboxylase in ventromedial prefrontal cortex. Proc Natl Acad Sci USA 109: 7493-7498, 2012.
27. Dai YB, Tan XJ, Wu WF, *et al*: Liver X receptor beta protects dopaminergic neurons in a mouse model of Parkinson disease. Proc Natl Acad Sci USA 109: 13112-13117, 2012.
28. Noghero A, Perino A, Seano G, *et al*: Liver X receptor activation reduces angiogenesis by impairing lipid raft localization and signaling of vascular endothelial growth factor receptor-2. Arterioscler Thromb Vasc Biol 32: 2280-2288, 2012.
29. Pencheva N, Buss CG, Posada J, *et al*: Broad-spectrum therapeutic suppression of metastatic melanoma through nuclear hormone receptor activation. Cell 156: 986-1001, 2014.
30. Jackson A, O'Connor JP, Parker GJ and Jayson GC: Imaging tumor vascular heterogeneity and angiogenesis using dynamic contrast-enhanced magnetic resonance imaging. Clin Cancer Res 13: 3449-3459, 2007.
31. Koh DM, Blackledge M, Collins DJ, *et al*: Reproducibility and changes in the apparent diffusion coefficients of solid tumours treated with combretastatin A4 phosphate and bevacizumab in a two-centre phase I clinical trial. Eur Radiol 19: 2728-2738, 2009.